Developmental Biology 386 (2014) 321–330

Contents lists available at ScienceDirect

Developmental Biology

journal homepage: www.elsevier.com/locate/developmentalbiology

Identification of ELF3 as an early transcriptional regulator of human urothelium ☆

Matthias Böck [a], Jennifer Hinley [b], Constanze Schmitt [a], Tom Wahlicht [b], Stefan Kramer [c,1], Jennifer Southgate [b,*,1]

[a] Institute of Computer Science I12, Technische Universität München, Boltzmannstr. 3, 85748 Garching, Germany
[b] Jack Birch Unit for Molecular Carcinogenesis, Department of Biology, University of York, York YO10 5DD, UK
[c] Institute of Computer Science, Johannes Gutenberg-Universität Mainz, Staudingerweg 9, 55128 Mainz, Germany

ARTICLE INFO

Article history:
Received 31 July 2013
Received in revised form
13 December 2013
Accepted 18 December 2013
Available online 25 December 2013

Keywords:
Differentiation
Normal Human Urothelium
Microarray analysis
Time series
Gene expression
ELF3
PPARγ

ABSTRACT

Despite major advances in high-throughput and computational modelling techniques, understanding of the mechanisms regulating tissue specification and differentiation in higher eukaryotes, particularly man, remains limited. Microarray technology has been explored exhaustively in recent years and several standard approaches have been established to analyse the resultant datasets on a genome-wide scale. Gene expression time series offer a valuable opportunity to define temporal hierarchies and gain insight into the regulatory relationships of biological processes. However, unless datasets are exactly synchronous, time points cannot be compared directly.

Here we present a data-driven analysis of regulatory elements from a microarray time series that tracked the differentiation of non-immortalised normal human urothelial (NHU) cells grown in culture. The datasets were obtained by harvesting differentiating and control cultures from finite bladder- and ureter-derived NHU cell lines at different time points using two previously validated, independent differentiation-inducing protocols. Due to the asynchronous nature of the data, a novel ranking analysis approach was adopted whereby we compared changes in the amplitude of experiment and control time series to identify common regulatory elements. Our approach offers a simple, fast and effective ranking method for genes that can be applied to other time series.

The analysis identified ELF3 as a candidate transcriptional regulator involved in human urothelial cytodifferentiation. Differentiation-associated expression of ELF3 was confirmed in cell culture experiments and by immunohistochemical demonstration in situ. The importance of ELF3 in urothelial differentiation was verified by knockdown in NHU cells, which led to reduced expression of FOXA1 and GRHL3 transcription factors in response to PPARγ activation. The consequences of this were seen in the repressed expression of late/terminal differentiation-associated uroplakin 3a gene expression and in the compromised development and regeneration of urothelial barrier function.

Introduction

The bladder and associated lower urinary tract is lined by urothelium, a transitional epithelium that functions as a permeability barrier to limit exposure to urinary toxins and to minimise alterations in urine and blood composition ((Fellows and Marshall, 1972); reviewed (Lewis, 2000)). The maintenance of this vital urinary barrier is supported by an exceptional regenerative capacity, whereby the urothelium switches from a mitotically-quiescent to a highly proliferative state in response to damage (Lavelle et al., 2002).

Urothelium shows an increase in morphological complexity between basal, intermediate and superficial cell zones. The lumen-facing superficial cells are uniquely specialised to provide urinary barrier function. With well-developed tight junctions limiting paracellular permeability (Varley et al., 2006), the major transurothelial barrier is provided by thickened plaques of asymmetric unit membrane (AUM) decorating the apical membrane of the superficial cells (Hicks, 1965). The AUM is constituted in the Golgi as a result of precise uroplakin protein interactions (reviewed (Wu et al., 2009)), the disruption of which has devastating consequences for urothelial permeability and urinary tract development. Thus, the targeted disruption of the uroplakin UPK3a gene in mice resulted in distinctive structural and functional

☆Data availability: Microarray data are available in the ArrayExpress database (www.ebi.ac.uk/arrayexpress) under accession number E-MTAB-2188.

* Corresponding author.
E-mail address: jennifer.southgate@york.ac.uk (J. Southgate).

[1] Equal contributions

0012-1606/$ - see front matter © 2014 Elsevier Inc. All rights reserved.
http://dx.doi.org/10.1016/j.ydbio.2013.12.028

abnormalities of the urothelium and high grade vesicoureteric reflux (Hu et al., 2002). Although a few examples of minor uroplakin gene anomalies associated with urinary tract malformations have since been found in man (Jenkins et al., 2005), there is no common association (Garthwaite et al., 2006; Giltay et al., 2004; Jiang et al., 2004; Kelly et al., 2005), indicating that major disruption of urothelial differentiation during human development is likely non-viable.

Although morphological and molecular features of urothelial differentiation are well characterised, relatively little is known of the transcriptional mechanisms underpinning this process. In mice, Kruppel-like factor 5 (KLF5) has been shown to be involved in the embryological development and differentiation of bladder urothelium (Bell et al., 2011). In the same study, KLF5-null foetal urothelium was shown to be deficient for expression of PPARγ, GRHL3, ELF3 and OVOL1, supporting the participation of these factors in a hierarchical transcriptional network regulating urothelial development. The authors further showed in transient transfection assays that KLF5 regulated expression of the mGRHL3 promoter. In mouse development, GRHL3 plays an essential role in epidermal morphogenesis, with GRHL3-deficient mice exhibiting failed skin barrier formation, defective wound repair and loss of eyelid fusion (Boglev et al., 2011). GRLH3 has also been shown to be critical to urothelial differentiation during mouse development (Yu et al., 2009). Although it is assumed that these factors and relationships are conserved from mouse to man, there is a lack of experimental approach to enable these developmental relationships to be assessed in human cells.

We have developed a robust experimental system for the propagation and differentiation of normal human urothelial (NHU) cells in vitro. When isolated from the tissue and cultured in a serum-free low calcium medium as finite cell lines, NHU cells subsume a basal squamous (CK14+) phenotype, are highly proliferative and do not show spontaneous differentiation even at confluence (Southgate et al., 1994). Nevertheless, cultured NHU cells retain the capacity to differentiate to form a functional barrier urothelium, as shown by subculture in medium containing bovine serum and physiological [Ca^{2+}], where transepithelial electrical resistances of $>3000\,\Omega\,cm^2$ are routinely attained (Cross et al., 2005). In addition, pharmacological activation of the nuclear receptor peroxisome proliferator activated receptor gamma (PPARγ) initiates the urothelial differentiation gene expression programme in individual cells, but without self-organisation into a barrier urothelium (Varley et al., 2004a, 2004b, 2006, 2009). Thus, the outcomes of these two differentiation-inducing protocols are not identical, yet both result in development of a differentiated urothelial cell phenotype. We reasoned that comparison of the two protocols to identify common changes in gene expression over time would help limit method-dependent artefacts and hence was a strategy that could help identify key regulatory genes involved in determining urothelial differentiation.

To these ends, we performed a gene array series at different time-points following differentiation induction using the two differentiation-inducing protocols performed in parallel. Our aim was to perform an unbiased analysis to identify common regulatory features and in the following, we describe the quality assessment of the data, the overcoming of synchronisation issues by performing a qualitative ranking approach, the identification of a set of significant genes involved in transcriptional regulation and the experimental validation of a previously unidentified regulator of human urothelial cytodifferentiation.

Materials and methods

Troglitazone (TZ) was obtained from Sigma-Aldrich (Dorset, UK) and the EGF receptor tyrosine kinase inhibitor PD153035 was obtained from Merck Millipore (Darmstadt, Germany). The PPARγ-specific antagonist, T0070907 was obtained from Cambridge Bioscience (Cambridge, UK). Rabbit anti-ELF3 antibody (ab97310) was obtained from Abcam, Cambridge, UK. Mouse anti-β-actin (clone AC-15) was obtained from Sigma-Aldrich (Dorset, UK).

Tissue samples

Human urothelial tissue samples were sourced ethically with informed written consent from patients and approval for use in research from Leeds (East) and York Research Ethics Committees. The surgical specimens were collected from patients with no history of urothelial cancer and were processed for histology or used to establish urothelial cell cultures. Samples taken for (immuno)histology were fixed for 16 h in 10% (v/v) formalin, dehydrated and processed into paraffin wax.

Cell culture

Finite NHU cell lines were established as detailed elsewhere (Southgate et al., 2002). For routine propagation, cultures were maintained as monolayers in low calcium [0.09 mM] Keratinocyte Serum Free Medium containing bovine pituitary extract and EGF (Invitrogen) and further supplemented with cholera toxin (KSFMc). Cultures were sub-cultured by trypsinisation at just-confluence and used for experiments between passages 3 to 5.

To induce differentiation, two previously described methods were applied to just-confluent NHU cell cultures. In the first (referred to as TZ/PD), cultures were treated with 1 μM TZ with concurrent 1 μM PD153035 to block EGFR activation and induce individual cell differentiation (Varley et al., 2004a). In the second protocol (referred to as ABS/Ca^{2+}), cultures were pre-treated with 5% adult bovine serum (ABS, Harlan Sera-Lab) for 3 days before subculture (time point $T=0$ h) into KSFMc supplemented with 5% ABS and 2 mM $CaCl_2$, leading to generation of a differentiated, tight barrier epithelium as described (Cross et al., 2005). Vehicle control non-differentiated cultures were maintained in parallel in KSFMc and used at the same time points (between 24 h to 144 h). Cultures were lysed in situ with TRIzol® to prepare RNA by the manufacturer's recommended protocol (Invitrogen). RNA samples were treated with a DNA-free kit (Ambion) and quantified by UV spectrophotometry.

Microarray experiments and preprocessing

Time series experiments were performed on two independent donor NHU cell lines (Y579 and Y676) using the TZ/PD and ABS/Ca^{2+} differentiation-inducing protocols described above. For each arm of the experiment, parallel non-differentiated control cultures were included and RNA was extracted at 6, 24, 72 and 144 h, where $t=0$ coincided with the treatment to induce differentiation in the TZ/PD cultures. The nature of the differentiation process meant that (as described above and (Cross et al., 2005)) the ABS/Ca^{2+} arm had a serum pre-treatment stage, which affected absolute synchronisation of the two arms of the experiment. Following RNA extraction, induction of differentiation in the experimental arms was verified by assessing the expression of UPK2 transcript by quantitative real time PCR (not shown).

For the arrays, mRNA was converted to cDNA and then to biotin-labelled cRNA before hybridising to HG-U133 Plus 2.0 arrays (Affymetrix). The array chips were washed and scanned at 560 nm using an Affymetrix GeneChip Scanner. Quality assessment of the microarrays was performed with the arrayQualityMetrics package (Kauffmann et al., 2009) and two samples were discarded due to quality issues (one control sample: 72 h ABS/Ca^{2+} from cell line

Y676; and one experimental sample: 6 h TZ/PD from cell line Y676). The experiment thus yielded 30 arrays (2 cell lines × (2 experimental and 2 control arms) × 4 time points) − 2 discarded arrays).

All calculations were performed in *R*. The microarray data were RMA normalised (Irizarry et al., 2003) using the Bioconductor package affy (Gautier et al., 2004). To reduce the dimensionality of the data and to filter out insignificant signals, an intensity filter was applied, which retained probe sets for which at least 25 per cent of all time points for the experimental time series had an intensity above $\log_2(100)$. 25,461 probe sets remained after the filtering step, corresponding to about 13,500 genes. Since the time series began at 6 h, the first control time point was used as a zero time point to account for changes of the expression level between the starting point of the control cell lines and the experiments. This left three time series with five time points and one with four because of the discarded sample (the 6 h time point in the TZ/PD Y676 experiment). The quality analysis and a principal component analysis of the different samples are provided in the Supplementary Materials (S1–S5). An interactive visualisation of the results can be accessed from http://infosys.informatik.uni-mainz.de/research/timeseries-visualisation/downloads.

Filtering and ranking

We developed an approach that focused on the expression changes over time on a qualitative level to overcome the lack of precise synchronisation of events. We searched only for the maximum changing event per gene and experiment, and globally compared changes over time from control to experiment, thus avoiding the direct comparison of time points. We calculated for each probe set time series a ΔX, the difference between the maximum intensity of all time points $x_i \in X$ (with i being the time point one to five, including the first control time point as zero time point) to the minimum intensity of all time points

$$\Delta X = max(x_i \in X) - min(x_j \in X) \quad (1)$$

This difference ΔX describes the maximum change over time per probe set for each time series. In a second step, we calculated the difference of the scale120%Δscale100%X_{exp} for the experiment and the scale120%Δscale100%X_{ctrl} for the control time series. We refer to this as the amplitude log fold change (ALFC):

$$ALFC = \text{scale120\%}\Delta\text{scale100\%}X_{exp} - \text{scale120\%}\Delta\text{scale100\%}X_{ctrl} \quad (2)$$

This value defines if a probe set changes significantly over time compared to its control, without having to compare the individual time points. A positive ALFC means the change is larger for the experiment and a negative value vice versa, indicating a silenced gene. Probe sets were then ordered in decreasing order of their ALFC value.

Validation experiments

In validation experiments, NHU cell cultures (independent cell lines from arrays) were induced to differentiate by co-treatment with 1 μM TZ and 1 μM PD153035 as described above and in (Varley et al., 2004a). To further define the role of PPARγ, parallel cultures were pretreated for 3 h with 5 μM T0070907 as a specific PPARγ antagonist prior to induction of differentiation. Replicate cultures were harvested at 6, 24, 48 and 72 h and used to extract DNA-free RNA for analysis of transcript expression (see below). Parallel cultures were lysed and processed for immunoblotting and probed with rabbit anti-ELF3 antibody, which was also used to assess ELF3 localisation in paraffin wax-embedded tissue sections of human urothelium by immunoperoxidase histochemistry (see below). Appropriate vehicle (DMSO), loading (β-actin for RT-PCR and immunoblotting) and specificity (RT-negative and irrelevant antibody) controls were included in all experiments.

Reverse-transcribed (RT) and real-time quantitative (RTq) PCR.

Cell cultures were solubilised in TRIzol® and the RNA was isolated by chloroform extraction and iso-propanol precipitation, according to the manufacturer's protocol (Life Technologies, Paisley, UK). The RNA was treated with DNase I (DNA-free™ kit from Ambion, Huntingdon, UK). cDNA was synthesised from 1 μg of total RNA using the Superscript first-strand synthesis system (Life Technologies, Paisley, UK). RT-PCR was performed using Go Taq® Hotstart Polymerase (Promega, Southampton, UK) with primer sets designed to amplify specific human products (Table 1). RT negative and no template (water) controls were always included.

For semi-quantitative analysis, template cDNA was mixed with SYBR® Green PCR Master Mix (Applied Biosystems) and 300 nM of each forward and reverse target gene primers (Table 1) and analysed on an ABI StepOnePlus™ Real Time PCR System. The thermal profile was: 20 s hold at 95 °C, followed by 40 cycles of denaturation at 95 °C (3 s) and elongation at 60 °C (30 s). Dissociation curves were performed to confirm the presence of a single amplification product and the absence of primer dimers for each primer set. Assay efficiency, validated using the CT slope method prior to use, confirmed that both the test and endogenous assays were of equivalent efficiency (within tolerance range). SYBR® Green results were expressed as relative quantification (RQ) values (Applied Biosystems).

Immunohistochemistry

De-waxed 5 μm tissue sections were blocked for endogenous peroxidase activity with 3% (v/v) hydrogen peroxide for 10 min. Antigen retrieval was performed by microwave boiling of tissue sections in a 10 mM citric acid buffer (pH 6.0) for 10 min, followed by 10 min cooling on ice. Tissue sections were treated with an Avidin/Biotin blocking kit (Vector labs, Peterborough, UK), before

Table 1
Primer sequences used for RTPCR and RTqPCR.

PCR product (gene name)	Forward primer (5′–3′)	Reverse primer (5′–3′)
ELF3 (RTPCR)	GTTCATCCGGGACATCCTC	GCTCAGCTTCTCGTAGGTC
ELF3 (RTqPCR)	TCAACGAGGGCCTCATGAA	TCGGAGCGCAGGAACTTG
GRHL3 (RTqPCR)	TGGAATATGAGACGGACCTCACT	CAGACACGTTCTCTGTCAGGAATT
FOXA1 (RTqPCR)	CAAGAGTTGCTTGACCGAAAGTT	TGTTCCCAGGGCCATCTGT
UPK3a (RTPCR)	CGGAGGCATGATCGTCATC	CAGCAAAACCCACAAGTAGAAAGA
UPK2 (RTqPCR)	CAGTGCCTCACCTTCCAACA	TGGTAAAATGGGAGGAAAGTCAA
CLDN7(RTqPCR)	GCAGTGGCAGATGAGCTCCTAT	CATCCACAGCCCCTTGTACA
β-actin (RTPCR)	ATCATGTTTGAGACCTTCAA	CATCTCTTGCTCGAAGTC
GAPDH (RTqPCR)	CAAGGTCATCCATGACAACTTTG	GGGCCATCCACAGTCTTCTG

applying 10% goat serum for 5 min to prevent non-specific binding of the secondary antibody. Rabbit anti-ELF3 antibody (2 μg/ml) was applied, followed by biotinylated goat anti-rabbit secondary antibody (1/800, Dako Cytomation Ltd, Ely, UK) – each for 15 min at ambient temperature, with washing in between. Antibody binding was detected using a tyramide-based signal amplification system (CSA system, Dako Cytomation Ltd, Ely, UK), as described in the manufacturer's protocol. Tissues were lightly counterstained in Mayer's haematoxylin, dehydrated through ethanol to xylene and mounted in DPX (Sigma Aldrich).

Immunoblotting

Culture lysates were resolved on 4–12% gradient bis-Tris acrylamide NuPAGE® gels (Life Technologies, Paisley, UK) and electrotransferred onto 0.45-μm PVDF-FL membranes (Merck Millipore, Darmstadt, Germany). Membranes were probed with anti-ELF3 (1 μg/ml) and β-actin (1/250,000) antibodies for 16 h at 4 °C; bound antibody was detected with goat anti-rabbit Ig conjugated to IRDye® 800 (50 ng/ml; Rockland Immunochemicals; supplied by Tebu-bio, Peterborough, UK) or anti-mouse immunoglobulins conjugated to Alexa Fluor® 680 (200 ng/ml; Life Technologies), as appropriate. Immunolabelled protein bands were visualised and relative quantifications generated using an Odyssey infrared imaging system (LiCor, Cambridge, UK).

Knock-down of ELF3 by retroviral-mediated shRNA interference

For RNA interference experiments, siRNA oligos were designed to target the ELF3 coding sequence before adding the hairpin loop, restriction overhangs for directional cloning and an Mlu1 restriction site (to verify cloned inserts) to generate the following ELF3 sense shRNA sequences including hairpin loop:

shRNA1: GATCCGCTACCAAGTGGAGAAGAACATTCAAGAGATGTTCTTCTCCACTTGGTAGCTTTTTTACGCGTG

shRNA2:

GATCCGCTCTTCTGATGAGCTCAGTTTTCAAGAGAAACTGAGCTCATCAGAAGAGCTTTTTTACGCGTG

shRNA3:

GATCCGCTCAGTTGGATCATTGAGCTTTCAAGAGAAGCTCAATGATCCAACTGAGCTTTTTTACGCGTG

Oligonucleotides were annealed and cloned into the RNAi-Ready pSIREN-RetroQ retroviral expression vector (Clontech) and transfected into the PT67 packaging cell line using the manufacturer's protocols. An irrelevant shRNA was also prepared using the control sequence provided by Clontech. Following antibiotic selection, conditioned virion-containing medium was harvested from confluent PT67 cultures and filtered through a 0.45 μm low protein binding Tuffryn® filter to remove cell debris. NHU cells were transduced for 6 hr with 8 ml of conditioned medium supplemented with 8 μg/ml Polybrene (Hexadimethrine Bromide, Sigma), after which virus-containing medium was removed and cultures replenished with KSFMc. Transduced NHU cell cultures were selected with 1 μg/ml puromycin and screened for ELF3 protein expression by immunoblotting following induction of differentiation.

Transepithelial electrical resistance (TER) studies

Differentiating urothelial cell cultures were established on Snapwell™ membranes using the ABS/Ca^{2+} differentiation-inducing protocol and with medium changed on alternative days. TER readings were taken daily using a portable EVOM™ Epithelial Volt-ohmmeter (World Precision Instruments), as described (Rubenwolf and Southgate, 2011).

After stabilisation of the TER readings, cultures were scratched to create a wound of 250 μm wide. Further TER measurements were taken at regular intervals over a period of 61 h during wound closure.

Results

Candidate gene selection

The time series microarray data was pre-processed and filtered as described in the Methods section. The first intensity filtering left 25,461 probe sets (about 13,500 genes). The initial goal was to prioritise and group genes with respect to their possible importance in regulating the differentiation or proliferation process. The main difficulty for the analysis of the time series data arose due to inherent (a) variability between the two biological replicates (independent human donor cell lines) studied and (b) differences in the pre-treatment and hence precise timing of the two procedures (ABS/Ca^{2+} and TZ/PD) used to induce differentiation. Together, these confounded synchronisation of the experimental arms and impaired direct comparison of control and experimental time points. To overcome these issues, we developed an approach that focused on the expression changes over time on a qualitative level, which we refer to as the ALFC. Thus, instead of performing pairwise comparisons between each time point of control and experiment, we looked for the maximum expression burst in the time series for each gene and compared the global expression change over time between the control and experiment. By discretising the global differences between experimental and control arms, we effectively circumvented any problems related to shifts in timing between or within experiments. The result was that we were able to avoid direct comparison of the time points, whilst still considering the time information. An overview of the resulting sets and their intersections is shown in Fig. 1.

The calculated ALFC was then used for further filtering of the data sets. We used a set of 25 pre-defined marker genes selected as implicated in urothelial differentiation or proliferation (Table 2) in order to select the size of sets for further investigation. Fig. 2 shows the stair-step plots with the number of markers included by applying different thresholds for each of the four experimental arms (see Table 3 for an overview of the included markers). Based on this analysis, we selected the top 1000 ranked probe sets associated with each experimental arm. We proceeded to analyse the different intersections between the four selected top 1000 probe sets (see Fig. 1A and B for an overview). By definition, the overlap between all four experimental arms (two biological replicates and two differentiation-inducing procedures) identified common (method-independent) genes, whereas the overlap exclusive to either of the two differentiation-inducing procedures (ABS/Ca^{2+} or TZ/PD) revealed method-dependent factors.

Identification of common regulatory genes implicated in urothelial differentiation.

For the intersection of all four sets, the ALFC was normalised to one for each experimental arm and the absolute sum of the ALFC was calculated and used to prioritise the list of probe sets. The overlap of all four experiments resulted in 189 probe sets and the overlap of the ABS/Ca^{2+} arms resulted in 427 probe sets (see Fig. 1C and D). The 20 top ranked genes on these lists are shown in Table 4. We next used the dragon TcoF-DB (Schaefer et al., 2011) to find transcription factors (TFs) of interest within the two sets. TcoF-DB currently consists of 1365 TFs which were manually curated (Vaquerizas et al., 2009) or are contained in TRANSFAC, where they have passed a manual curation step.

Four TFs (ELF3, BNC1, BCL6 and IRF1) were found in the overlap of all four experiments and 13 TFs were associated with the ABS/Ca^{2+}

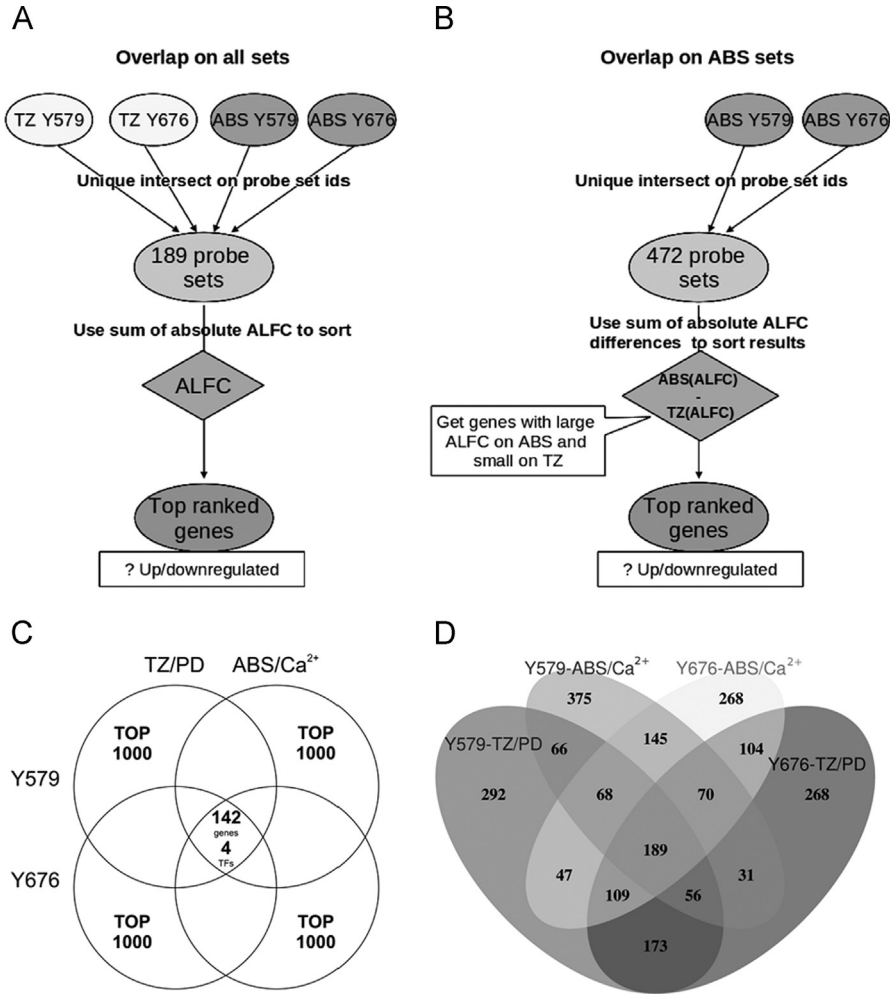

Fig. 1. Overview of the probe set overlaps between the experiments. Figures A and B give an overview of how the top ranked probe sets were combined. The intersection was built either on all four filtered 1000 top ranked sets or the two ABS/Ca^{2+} experimental arms. The ALFC for each probe set was then normalised to one and the set sorted according to the sum of absolute ALFC over all experiments. The intersection of the ABS/Ca^{2+} sets was ranked from the difference between the absolute sum of ALFC on the ABS/Ca^{2+} arm and the absolute sum of the ALFC on the TZ/PD arm. Figures C and D display Venn diagrams which show the intersection and overlaps of the four differentiation series (TZ/PD and ABS/Ca^{2+}, on two independent donor cell lines Y579 and Y676). The overlaps were generated using the top 1000 probe set lists from each experiment; probe sets were used in order to keep the gene lists as accurate as possible and to enable tracking back to the specific probe sets on the microarray which are contained in our final lists. The Venn diagram in panel C shows the number of genes present at the intersection of all four data sets. 142 up-/downregulated genes were found within the intersection. Within this subset, four TFs were found (ELF3, BCL6, BNC1, IRF1). Figure D shows the same overlaps on the probe set level. The 189 probe sets in the intersection of all sets map to the 142 genes from Figure C. The overlap between the ABS/Ca^{2+} experimental arms contains 472 probe sets with 13 identified as TFs (see Table 2 for details). From these 13 TFs, nine factors (GRHL1, GRHL3, FOXC1, ID2, SMAD3, FOXN2, ETS1, MITF and FOXD1) were unique to the ABS/Ca^{2+} arm and not included in the TZ/PD lists.

Table 2
List of markers for probe set filtering.

Expected expression versus control	Marker genes
Expressed, but not expected to change	KRT7, KRT19, GAPDH, ACTB, SMAD2,
Downregulated	KRT5, KRT6A, KRT6B, SMURF2, SMAD7, MYBL2, BUB1, PLK1, CREB1
Upregulated early	FOXA1, GATA3, IRF1, IRF2
Upregulated late	KRT13, CLDN4, UPK2, UPK3A, UPK1A, UPK1B, UPK3B

This list gives an overview of the proliferation and differentiation-associated transcribed gene markers used to define the filtering thresholds.

overlap, of which nine TFs (GRHL1, GRHL3, FOXC1, ID2, SMAD3, FOXN2, ETS1, MITF and FOXD1) remained after the TZ/PD arm was filtered out. It should be noted that the gene list for the ABS/Ca^{2+} overlap does not necessarily exclude a gene from being also relevant to the TZ/PD model: the list contains similar genes but the specific ranking is based only on the ABS/Ca^{2+} arm.

ELF3 was the top ranked TF (overlap of all sets) with a larger ALFC value than most other genes in all four differentiated datasets (see Fig. 3). The 95% quantile of all probe sets (in the overlap of all sets) lay at an ALFC value of 0.6, while the three probe sets for ELF3 represented on the HG-U133 Plus 2.0 chip (210827_s_at, 229842_at, 201510_at) reached values of 1.57, 2.06 and 1.72, respectively. A two-tailed *p*-value test for all three probe sets was significantly smaller than 0.05 (between 2.6e-10 and 5.3e-18). The main expression burst for ELF3 occurred early, between 0 h to 24 h, and increased in the case of the TZ/PD arm until 72 h. As ELF3 has not been previously implicated in human urothelial cytodifferentiation, we validated its expression in human urothelium in situ and during differentiation of normal human urothelial cells in vitro. In addition, we examined how the expression of ELF3 was regulated in relationship to PPARγ activation.

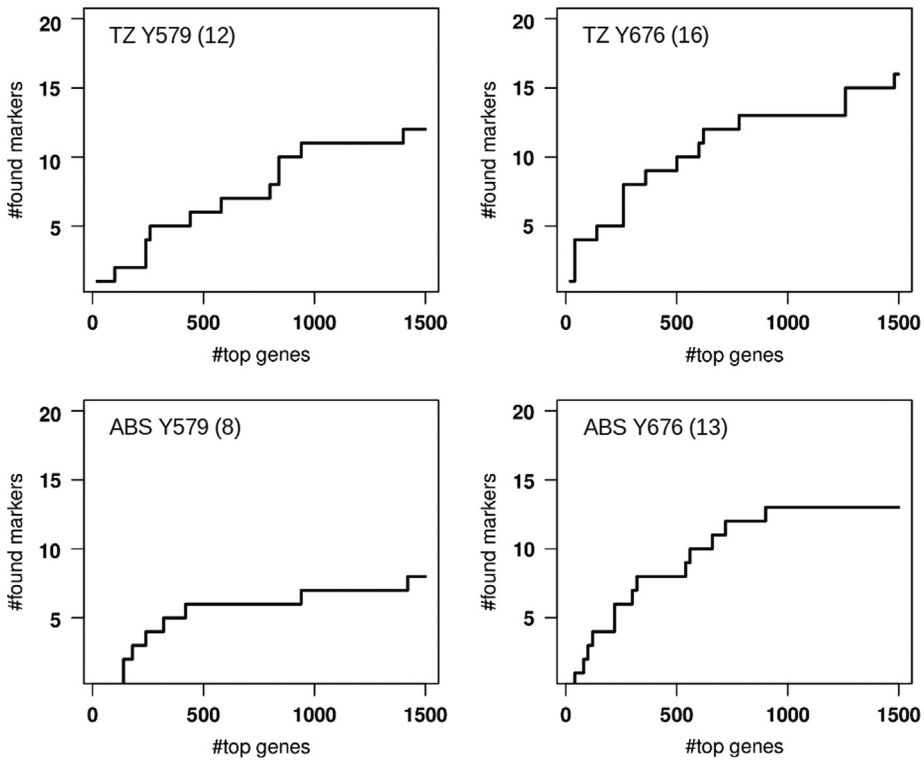

Fig. 2. Defining the ALFC threshold. Stair-step plots for the four experiments showing the number of rediscovered markers in the data set for differently sized sets of top ranked probe sets (up to 1500). The ranking was performed using the calculated ALFC and each bar represents the number of found markers for the particular amount of chosen genes. A plateau around 1000 is reached in all four data sets and hence a threshold of choosing the top 1000 probe sets was applied for the second filtering step. The maximum amount of found markers is shown in brackets next to the experiment identifier in the left corner of each chart.

Table 3
Overview of top ranked probe sets and their associated marker genes.

Experimental arm (cell line)	Probe sets (No. of genes represented)	No. genes		Marker genes
		+	−	
TZ/PD (Y579)	1000 (707)	955	45	UPK1A, UPK1B, UPK2, UPK3A, IRF1, FOXA1, CLDN4, KRT5/6A/6B, SMAD7
TZ/PD (Y676)	1000 (695)	997	3	UPK1A, UPK1B, UPK2, UPK3A, UPK3B, ACTB, KRT5/6A/6B/13, IRF1, FOXA1, GATA3
ABS/Ca^{2+} (Y579)	1000 (731)	953	47	UPK1B, KRT5/6A/6B/13, IRF1, CLDN4
ABS/Ca^{2+} (Y676)	1000 (755)	996	4	UPK1A, UPK1B, UPK3A, UPK3B, IRF1, SMAD7, SMURF2, KRT5/6A/6B/13, CLDN4, FOXA1, GATA3

This Table gives an overview of the four experiments with the top 1000 ranked probe sets (number of genes represented) according to ALFC and showing the associated marker genes (from Table 2). Genes were assigned as positive (+) or negative (−) depending on the ALFC value. A positive ALFC value indicates that over the time series, the gene expression of the probe set for the experimental arm changed more than for the control arm.

Table 4
Overview of TFs and 20 top ranked genes within the overlaps of the experiments.

Overlap of all sets		Overlap of ABS/Ca^{2+} experiments	
TFs	**Top 20**	**TFs**	**Top 20**
ELF3, BNC1, BCL6, IRF1	RARRES1, LIMCH1, TRIM31, UBD, SPINK1, PDE10A, TMPRSS2, CP, PIGR, C10orf116, HPGD, CX3CL1, GKN1, IGFBP3, ELF3, RHOU, SYTL5, TFF1, MUC20, RARRES3	GRHL1, GRHL3, FOXC1, ID2, BNC1, SMAD3, ELF3, BCL6, FOXN2, ETS1, IRF1, MITF, FOXD1	MUC4, CLIC5, CXCL6, BCL2A1, DUOX2, SERPINB9, SERPINA3, PIGR, MAP3K8, IDO1, IL1RL1*, ZG16B, IL8, PDZRN3, RARRES3, MMP7, GABRP*, PPBP*, RARRES1

This table shows the lists of top ranked genes in the overlaps/intersections of all four experimental arms and for the two ABS/Ca^{2+} specific arms (see Fig. 2C and D). The genes are ordered according to their ALFC. We observe for the TZ/PD model the largest gene expression burst between 24 h and 72 h. For the ABS/Ca^{2+} model, the burst occured earlier, between 0 h and 6 h (but note that this protocol involves a priming pre-treatment). *The majority of the genes are up-regulated, except the genes IL1RL1, GAPRP and PPBP from the overlap of the ABS/Ca^{2+} arms.

Validation of ELF3 expression by human urothelium.

By immunohistochemistry, ELF3 localised specifically to the urothelium in sections of human ureter. The localisation pattern was exclusively nuclear and the intensity of expression increased from basal to the most differentiated superficial cells (Fig. 4A).

In cultures of NHU cells induced to differentiate by activation of PPARγ (through co-treatment with TZ and PD153035), ELF3

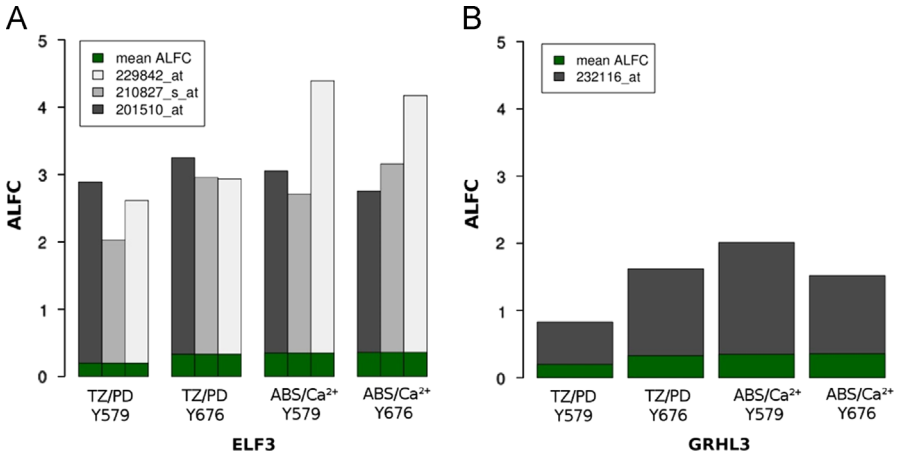

Fig. 3. ALFC values for ELF3 and GRHL3. ALFC values for the probe sets of two genes of interest, ELF3 and GRHL3. The mean ALFC of all probe sets is shown by the green bars. For the two genes the ALFC is significantly larger than for the average probe set.

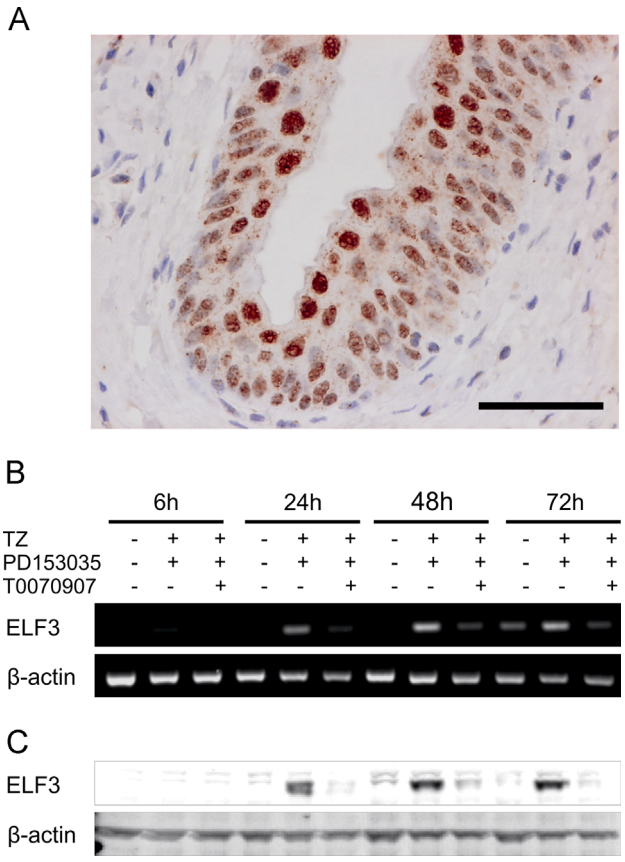

Fig. 4. Experimental validation of ELF3. ELF3 immunolocalisation in human urothelium on a section of normal ureter (A). Note nuclear localisation and increased intensity in the most highly differentiated superficial cells (Scale bar = 50 μM). Expression of ELF3 transcript (B) and protein (C) was examined in NHU cells induced to differentiate in response to the TZ/PD protocol. The antagonist T0070907 was used to confirm specific involvement of PPARγ. Cells were pre-treated with 5 μM T0070907 (or vehicle control) for 3 h prior to addition of 1 μM TZ and 1 μM PD153035. RNA extractions and whole-cell protein lysates were collected for analysis at 6, 24, 48 and 72 h post-treatment. At each time point a DMSO vehicle control was included. For transcript analysis (B), ELF3 gene expression was analysed by RT-PCR and β-actin was included as a normalisation control. Whole cell lysates were processed for western blotting (C) and labelled with antibodies against ELF3 or β-actin as loading control.

transcript expression was induced within 24 h and remained high at 72 h. Inhibition of PPARγ activation by pretreatment of cells with the specific PPARγ antagonist, T0070907, resulted in inhibition of ELF3 induction (Fig. 4B).

The ELF3 transcript results were confirmed by immunoblotting for ELF3 protein, which revealed upregulation of ELF3 protein at 24 h. Inhibition by pretreatment with T0070907 confirmed that this was a PPARγ-mediated process (Fig. 4C).

Immunoblotting revealed that retrovirally-transduced stable expression of shRNA against the ELF3 protein coding sequence was successful at inhibiting ELF3 protein expression following induction of differentiation by PPARγ activation. Of the three shRNA sequences tested, shRNA1 showed the most efficient knockdown and was used in subsequent experiments (Supplementary Materials S6). Following induction of differentiation in response to PPARγ activation (TZ/PD protocol), cells stably transduced with ELF3 shRNA1 showed reduced induction of ELF3 transcript and of the terminal differentiation-associated UPK3a gene, compared to the transduced control shRNA cells (Fig. 5A). Quantitative analysis by real-time PCR of the ELF3 knock-down cultures showed reduced differentiation-induced expression of CLDN7 and of the transcription factors FOXA1 and GRHL3 (Fig. 5B).

To assess the consequence of ELF3 knockdown on differentiated urothelial barrier function, TER was used to monitor barrier development post-induction of differentiation using the ABS/Ca^{2+} protocol. A measurable barrier first became apparent at four days post-induction of differentiation in both the control and ELF3 knockdown cells, but the ultimate TER attained was significantly reduced in the latter (control versus ELF3k/d: 3420 ± 443 versus $2061 \pm 176\ \Omega\ cm^2$; $p < 0.001$ $\pm$ sd; $n = 6$; Fig. 5C). Following scratch wounding of the cultures, initiation of barrier repair was less efficient and the final barrier attained was reduced in the ELF3 knockdown cells compared to the shRNA control transduced cells (Fig. 5D).

Discussion

Much has been learned about transcriptional regulation during tissue development from null expression studies in transgenic mice, but translation to human systems is more challenging. Here we demonstrate how bioinformatics analysis of a normal human differentiating cell culture time series can identify key transcriptional regulators involved in human tissue-specific determination and differentiation, and provide insight into the relationships and hierarchies of the transcriptional networks.

We have described a qualitative approach for the analysis of asynchronous time series data and applied it to four gene expression time series representing two differentiation-inducing protocols in bladder and ureter derived finite normal human urothelial

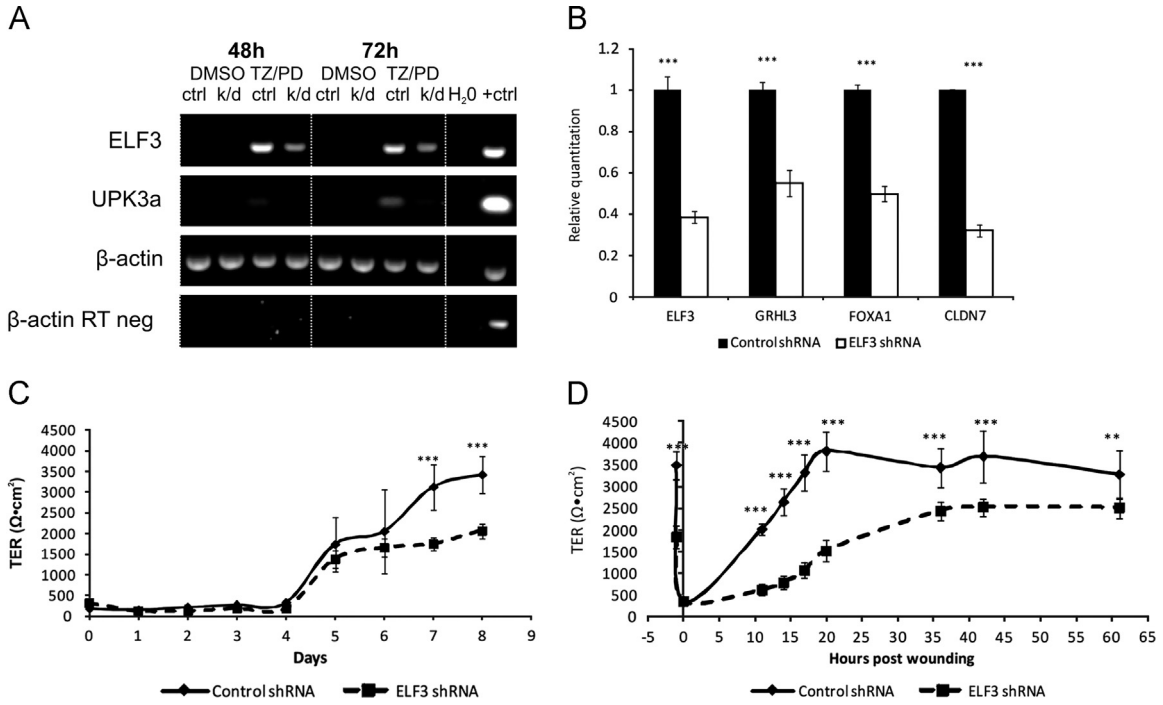

Fig. 5. Analysis of ELF3 knock-down on NHU cytodifferentiation and barrier repair. Expression of urothelial differentiation-associated genes was examined in ELF3 versus control shRNA transduced cells. (A) Scrambled shRNA control (ctrl) and ELF3 knockdown (k/d) cells cultures were exposed to vehicle only (0.1% DMSO) or differentiated by co-treatment with TZ and PD153035 (TZ/PD) and the expression of ELF3 and late differentiation-associated UPK3a was analysed by RT-PCR at 48 h and 72 h post-treatment. (B) The expression of ELF3, GRHL3, FOXA1 and claudin 7 was analysed by RTqPCR in cells transduced with control versus ELF3 shRNA at 48 h post differentiation with TZ/PD. In A and B, the reaction controls included an RT-negative for each RNA sample, a no-template (H_2O) control, a β-actin normalisation control and a genomic DNA positive control. (C) Barrier function in ELF3 versus control shRNA transduced cultures was followed over an 8 day period following differentiation in ABS/Ca^{2+} by measurement of the TER. D) The same cultures were then wounded and the restoration of barrier function was observed over the subsequent 61 h. Statistical analysis was calculated by ANOVA with Bonferroni Multiple Comparisons post-test (***$P<0.001$, **$P<0.01$).

cell lines. Unlike other methods for analysing short time series (Conesa et al., 2006; Zoppoli et al., 2010), our method is directly applicable to analysing non-synchronous short time series and overcomes issues of missing time points or replicates. The result of our analysis is a ranked list that offers an intuitive pipeline for successive iterations between data analysis and biological evaluation to attain a manageable set of candidate genes. The same approach can be used to look for specific differences between different experimental arms to identify genes upregulated by one protocol only. For example, such analyses could provide insight as to why the ABS/Ca^{2+} protocol generates a differentiated multi-layered and functional barrier urothelium, compared to the generation of differentiated but non-organised monolayer cell cultures that result from the TZ/PD protocol.

In this report, we concentrated on identifying common (method-independent) genes involved in regulating the development of a differentiated phenotype from normal human urothelial cells. The culture system is such that it maintains NHU cells in a proliferative squamous basal phenotype, characterised by $CK14^+$/$CK13^-$expression (Southgate et al., 1994) and we have shown that PPARγ activation (Varley et al., 2004a, 2004b, 2006) or subculture in serum (Cross et al., 2005) can switch cells into a differentiating $CK14^-$/$CK13^+$ transitional epithelial programme. Our analysis has identified the epithelium-specific Ets domain transcription factor ELF3 as a differentiation-associated gene whose expression is regulated downstream of PPARγ. In mice, ELF3 has been shown to be induced in the urothelium following infection with uropathogenic *Escherichia coli* (UPEC) (Mysorekar et al., 2002). Infection of the bladder epithelium of mice with UPEC triggers a response in which bacterial-laden superficial cells are exfoliated and the urothelium is reconstituted through differentiation of underlying basal and intermediate cells (Mysorekar et al., 2002). One of the early transcriptional responses to attachment of the UPECs is thought to be upregulation of the transcription factor ELF3, which has also been implicated in keratinocyte terminal differentiation (Andreoli et al., 1997; Oettgen et al., 1997). Mysorekar and colleagues hypothesised that ELF3 has a dual role in regulating urothelial differentiation and mediating host defence through transactivation of iNOS (Mysorekar et al., 2002). Targeted disruption of ELF3 in the mouse resulted in 30% lethality, with the remaining offspring reported as showing disrupted morphological and cellular differentiation of the small intestinal epithelium (Ng et al., 2002). ELF3-deficient enterocytes expressed markedly reduced levels of the transforming growth factor type II receptor (TGFβRII) and could be genetically rescued by introduction of a human TGFβRII transgene, demonstrating that Elf3 is the critical upstream regulator of TGFβRII in the mouse small intestinal epithelium (Flentjar et al., 2007). Transcriptional reprogramming of the TGFβR pathway, including downregulation of TGFβRII, has been documented in NHU cytodifferentiation (Fleming et al., 2012). However, TGFβR signalling was not associated in urothelial differentiation itself and instead was implicated in priming an autocrine tissue repair programme (Fleming et al., 2012).

A GRHL3-null mouse embryo model was used to demonstrate that the transcriptional regulator GRHL3 is required for formation of normal superficial cells and terminal differentiation of bladder urothelium (Yu et al., 2009). The gene and protein expression of the uroplakins was significantly downregulated in bladders of GRHL3-null mice and a functional GRHL3 binding site was identified on the UPK2 gene promoter. More recently it has been proposed that the transcriptional regulator KLF5 is required for urothelial maturation and differentiation (Bell et al., 2011). Thus, in mice with KLF5 deficient bladder epithelium, the urothelium fails to stratify and there was reduced expression of terminal

differentiation markers, including uroplakins and claudins. Eleven transcription factors were downregulated in KLF5-deficient bladder urothelium including PPARγ, ELF3, FOXA1 and GRHL3. The murine GRHL3 gene has been shown to be a downstream target of KLF5 and it has therefore been proposed that PPARγ and GRHL3 participate in a KLF5-dependent transcriptional network regulating urothelial differentiation (Bell et al., 2011).

We have previously shown a specific role for PPARγ in the induction of differentiation in normal human urothelial cell cultures, which depends both on the suppression of EGFR activity and availability of activating ligand (Varley et al., 2004a). PPARγ activation leads to de novo expression of intermediary transcription factors including FOXA1 and IRF1 that act directly as transcription factors for inducing the de novo expression of uroplakins and other genes associated with urothelial differentiation (Varley et al., 2009). ELF3 lies downstream of PPARγ: it has predicted PPAR response elements in the promoter and is induced specifically by PPARγ activation. We have now demonstrated that ELF3 influences urothelial differentiation, as the induction of UPK3a expression and the ultimate acquisition of barrier function were both inhibited by ELF3 knockdown. The effect on ELF3 on UPK3a transcription must be indirect as no Ets binding sites are predicted in the UPK gene promoters (not shown), although as shown by knockdown, ELF3 does influence expression of other implicated transcriptional regulators including FOXA1 and GRHL3.

In conclusion, we propose a hierarchy in the specification of human urothelium that has ELF3 downstream of PPARγ, but upstream of GRHL3 and FOXA1. We suggest that our strategy of studying the temporal development of a differentiated phenotype in vitro can help unravel the hierarchical relationships between candidate transcription factors and their individual roles in the differentiation programme and we have provided a new approach for extracting this information from gene array studies.

Funding

The bioinformatics work was supported by the DFG international research training group (IRTG) RECESS 1563 via scholarships to CS and MB. Experimental work was funded by York Against Cancer, who also supported JS and JH. The arrays were financed by GSK as part of an Industrial CASE studentship from the Biotechnology and Biological Sciences Research Council (BBSRC) that supported Jonathan M Fleming. TW was in receipt of an undergraduate internship from the Lausitz University of Applied Science, Germany, funded by the European Commission′s ERASMUS Lifelong Learning Programme.

Acknowledgements

The authors acknowledge Drs Claire Varley, Mary Garthwaite and Jonathan M Fleming from the Jack Birch Unit, University of York for generating the array data. Ms Shu Guo is thanked for generating the quantitative real-time PCR and TER data.

Appendix A. Supplementary materials

Supplementary data associated with this article can be found in the online version at http://dx.doi.org/10.1016/j.ydbio.2013.12.028.

References

Andreoli, J.M., Jang, S.I., Chung, E., Coticchia, C.M., Steinert, P.M., Markova, N.G., 1997. The expression of a novel, epithelium-specific ets transcription factor is restricted to the most differentiated layers in the epidermis. Nucl. Acids Res. 25, 4287–4295.

Bell, S.M., Zhang, L., Mendell, A., Xu, Y., Haitchi, H.M., Lessard, J.L., Whitsett, J.A., 2011. Kruppel-like factor 5 is required for formation and differentiation of the bladder urothelium. Dev. Biol. 358, 79–90.

Boglev, Y., Wilanowski, T., Caddy, J., Parekh, V., Auden, A., Darido, C., Hislop, N.R., Cangkrama, M., Ting, S.B., Jane, S.M., 2011. The unique and cooperative roles of the grainy head-like transcription factors in epidermal development reflect unexpected target gene specificity. Dev. Biol. 349, 512–522.

Conesa, A., Nueda, M.J., Ferrer, A., Talon, M., 2006. maSigPro: a method to identify significantly differential expression profiles in time-course microarray experiments. Bioinformatics 22, 1096–1102.

Cross, W.R., Eardley, I., Leese, H.J., Southgate, J., 2005. A biomimetic tissue from cultured normal human urothelial cells: analysis of physiological function. Am. J. Physiol. Renal Physiol. 289, F459–468.

Fellows, G.J., Marshall, D.H., 1972. The permeability of human bladder epithelium to water and sodium. Invest. Urol. 9, 339–344.

Fleming, J.M., Shabir, S., Varley, C.L., Kirkwood, L.A., White, A., Holder, J., Trejdosiewicz, L.K., Southgate, J., 2012. Differentiation-associated reprogramming of the transforming growth factor beta receptor pathway establishes the circuitry for epithelial autocrine/paracrine repair. PLoS One 7, e51404.

Flentjar, N., Chu, P.Y., Ng, A.Y., Johnstone, C.N., Heath, J.K., Ernst, M., Hertzog, P.J., Pritchard, M.A., 2007. TGF-betaRII rescues development of small intestinal epithelial cells in Elf3-deficient mice. Gastroenterology 132, 1410–1419.

Garthwaite, M.A., Thomas, D.F., Subramaniam, R., Stahlschmidt, J., Eardley, I., Southgate, J., 2006. Urothelial differentiation in vesicoureteric reflux and other urological disorders of childhood: a comparative study. Eur. Urol. 49 (154–159), 159–160.

Gautier, L., Cope, L., Bolstad, B.M., Irizarry, R.A., 2004. affy—analysis of Affymetrix GeneChip data at the probe level. Bioinformatics 20, 307–315.

Giltay, J.C., van de Meerakker, J., van Amstel, H.K., de Jong, T.P., 2004. No pathogenic mutations in the uroplakin III gene of 25 patients with primary vesicoureteral reflux. J. Urol. 171, 931–932.

Hicks, R.M., 1965. The fine structure of the transitional epithelium of rat ureter. J. Cell. Biol. 26, 25–48.

Hu, P., Meyers, S., Liang, F.X., Deng, F.M., Kachar, B., Zeidel, M.L., Sun, T.T., 2002. Role of membrane proteins in permeability barrier function: uroplakin ablation elevates urothelial permeability. Am. J. Physiol. Renal Physiol. 283, F1200–1207.

Irizarry, R.A., Hobbs, B., Collin, F., Beazer-Barclay, Y.D., Antonellis, K.J., Scherf, U., Speed, T.P., 2003. Exploration, normalization, and summaries of high density oligonucleotide array probe level data. Biostatistics 4, 249–264.

Jenkins, D., Bitner-Glindzicz, M., Malcolm, S., Hu, C.C., Allison, J., Winyard, P.J., Gullett, A.M., Thomas, D.F., Belk, R.A., Feather, S.A., Sun, T.T., Woolf, A.S., 2005. De novo Uroplakin IIIa heterozygous mutations cause human renal adysplasia leading to severe kidney failure. J. Am. Soc. Nephrol. 16, 2141–2149.

Jiang, S., Gitlin, J., Deng, F.M., Liang, F.X., Lee, A., Atala, A., Bauer, S.B., Ehrlich, G.D., Feather, S.A., Goldberg, J.D., Goodship, J.A., Goodship, T.H., Hermanns, M., Hu, F. Z., Jones, K.E., Malcolm, S., Mendelsohn, C., Preston, R.A., Retik, A.B., Schneck, F. X., Wright, V., Ye, X.Y., Woolf, A.S., Wu, X.R., Ostrer, H., Shapiro, E., Yu, J., Sun, T. T., 2004. Lack of major involvement of human uroplakin genes in vesicoureteral reflux: implications for disease heterogeneity. Kidney Int. 66, 10–19.

Kauffmann, A., Gentleman, R., Huber, W., 2009. arrayQualityMetrics—a bioconductor package for quality assessment of microarray data. Bioinformatics 25, 415–416.

Kelly, H., Ennis, S., Yoneda, A., Bermingham, C., Shields, D.C., Molony, C., Green, A.J., Puri, P., Barton, D.E., 2005. Uroplakin III is not a major candidate gene for primary vesicoureteral reflux. Eur. J. Hum. Genet. 13, 500–502.

Lavelle, J., Meyers, S., Ramage, R., Bastacky, S., Doty, D., Apodaca, G., Zeidel, M.L., 2002. Bladder permeability barrier: recovery from selective injury of surface epithelial cells. Am. J. Physiol. Renal Physiol. 283, F242–253.

Lewis, S.A., 2000. Everything you wanted to know about the bladder epithelium but were afraid to ask. Am. J. Physiol. Renal Physiol. 278, F867–874.

Mysorekar, I.U., Mulvey, M.A., Hultgren, S.J., Gordon, J.I., 2002. Molecular regulation of urothelial renewal and host defenses during infection with uropathogenic *Escherichia coli*. J. Biol. Chem. 277, 7412–7419.

Ng, A.Y., Waring, P., Ristevski, S., Wang, C., Wilson, T., Pritchard, M., Hertzog, P., Kola, I., 2002. Inactivation of the transcription factor Elf3 in mice results in dysmorphogenesis and altered differentiation of intestinal epithelium. Gastroenterology 122, 1455–1466.

Oettgen, P., Alani, R.M., Barcinski, M.A., Brown, L., Akbarali, Y., Boltax, J., Kunsch, C., Munger, K., Libermann, T.A., 1997. Isolation and characterization of a novel epithelium-specific transcription factor, ESE-1, a member of the ets family. Mol. Cell. Biol. 17, 4419–4433.

Rubenwolf, P., Southgate, J., 2011. Permeability of differentiated human urothelium in vitro. Methods Mol. Biol. 763, 207–222.

Schaefer, U., Schmeier, S., Bajic, V.B., 2011. TcoF-DB: dragon database for human transcription co-factors and transcription factor interacting proteins. Nucl. Acids Res. 39, D106–110.

Southgate, J., Hutton, K.A., Thomas, D.F., Trejdosiewicz, L.K., 1994. Normal human urothelial cells in vitro: proliferation and induction of stratification. Lab Invest. 71, 583–594.

Southgate, J., Masters, J.R., Trejdosiewicz, L.K., 2002. Culture of human urothelium. In: Freshney, R.I., Freshney, M.G. (Eds.), Culture of Epithelial Cells, (2nd Ed.) J Wiley and Sons, Inc., New York, pp. 381–400.

Vaquerizas, J.M., Kummerfeld, S.K., Teichmann, S.A., Luscombe, N.M., 2009. A census of human transcription factors: function, expression and evolution. Nat. Rev. Genet. 10, 252–263.

Varley, C.L., Bacon, E.J., Holder, J.C., Southgate, J., 2009. FOXA1 and IRF-1 intermediary transcriptional regulators of PPARgamma-induced urothelial cytodifferentiation. Cell Death Differ. 16, 103–114.
Varley, C.L., Garthwaite, M.A., Cross, W., Hinley, J., Trejdosiewicz, L.K., Southgate, J., 2006. PPARgamma-regulated tight junction development during human urothelial cytodifferentiation. J. Cell Physiol. 208, 407–417.
Varley, C.L., Stahlschmidt, J., Lee, W.C., Holder, J., Diggle, C., Selby, P.J., Trejdosiewicz, L.K., Southgate, J., 2004a. Role of PPARgamma and EGFR signalling in the urothelial terminal differentiation programme. J. Cell Sci. 117, 2029–2036.
Varley, C.L., Stahlschmidt, J., Smith, B., Stower, M., Southgate, J., 2004b. Activation of peroxisome proliferator-activated receptor-gamma reverses squamous metaplasia and induces transitional differentiation in normal human urothelial cells. Am. J. Pathol. 164, 1789–1798.
Wu, X.R., Kong, X.P., Pellicer, A., Kreibich, G., Sun, T.T., 2009. Uroplakins in urothelial biology, function, and disease. Kidney Int. 75, 1153–1165.
Yu, Z., Mannik, J., Soto, A., Lin, K.K., Andersen, B., 2009. The epidermal differentiation-associated grainyhead gene Get1/Grhl3 also regulates urothelial differentiation. EMBO J. 28, 1890–1903.
Zoppoli, P., Morganella, S., Ceccarelli, M., 2010. TimeDelay-ARACNE: Reverse engineering of gene networks from time-course data by an information theoretic approach. BMC Bioinf. 11, 154.